The Emergence of a Complex Representation of Touch Through Interaction with a Robot

Louis L'Haridon, Raphaël Bergoin, Baljinder Singh Bal, Mehdi Abdelwahed, Lola Cañamero

The emergence of a complex representation of touch through interaction with a robot

Louis L'Haridon[1], Raphaël Bergoin[1 2], Baljinder Singh Bal[1], Mehdi Abdelwahed[1], and Lola Cañamero[1]

[1] ETIS Lab (UMR 8051), CY Cergy Paris University / ENSEA / CNRS, Cergy-Pontoise, France
[2] Center for Brain and Cognition, Department of Information and Communications Technologies, Pompeu Fabra University, Barcelona, Spain
{louis.lharidon,raphael.bergoin,lola.canamero}@cyu.fr

Abstract. In this paper, we present a novel robot model of touch, and its representation in an artificial cortex, that aims to capture some of the complexity of human touch. In particular, our approach integrates artificial mechanoception and nociception in an adaptive sensory field (the robot's "sensory body"), allowing for a more comprehensive simulation of tactile sensations. The robot's sensory field is then processed by a biologically plausible neural network in a way akin to sensory processing in the somatosensory and anterior cingulate cortex. Findings from our experimental results show our model's ability to integrate complex data from infrared sensors, leading to the emergence of a spatial sensory body representation in our neural network, with potentially significant implications for robot perception and interaction.

Keywords: Adaptive Model of Touch and Pain · Bio-inspired Robotics · Computational Neuroscience · Neural network · Neurorobotics

1 Introduction

Touch is a sensory modality that allows organisms to perceive and respond to physical contact with their environment through specialized receptors in skin and other tissues. It is essential for constructing internal representations of the world, enabling the detection of noxious stimuli that signal harm. It also supports spatialization of the body helping to understand its position and movement in space. Touch perception involves sensory inputs such as mechanoception and nociception.

Mechanoception is the biological process through which the body perceives and interprets mechanical stimuli, including touch, pressure and vibration [27]. This process is mediated by sensory cells called mechanoreceptors [8] which are distributed through the skin, muscles and other tissues. These receptors respond to mechanical change, converting physical force into electrical signals transmitted through $A\beta$ fibers to the brain—specifically to the somatosensory cortex. The cortex processes and interprets the tactile sensation, enabling the construction of a physical body representation [9] (see, e.g., the *cortical homonculus* [28]).

Nociception is a biological process crucial for detecting potential or actual tissue damage [16]. It uses specific sensors, the nociceptors located in the skin, muscles, and organs, that detect harmful stimuli, triggering signals through nerve fibers, including $A\delta$ fibers for sharp pain, to the brain. Research in robotics has explored nociception models, incorporating nociceptors in robot designs for simulating pain detection mechanisms [19, 18].

This predefined pathway from sensory receptors to precise areas of the cortex could be at the origin of the brain's spatial and functional modular organization, where neurons and regions associated with common modalities or functions are more strongly connected [26]. More precisely, plasticity seems to shape these neural assemblies associated with specific sensory modalities or features within a modality, under the action of co-activation zones [12].

Building on Louis L'Haridon's PhD thesis on pain modeling in robots, and on Raphaël Bergoin's thesis on inhibitory plasticity in neural memory formation [4], the initial motivation for this study was to understand and model the emergence of a complex sensory representation of touch combining a new representation of mechanoception and nociception in a "sensory body" of a mobile robot, and a neural network model of the anterior cingulate cortex and somatosensory cortex in an immature brain (i.e. not having reached its definitive organization). More precisely, the aim is to model the pathway from nociceptors (respectively mechanoreceptors) associated with the skin, to the anterior cingulate cortex (respectively somatosensory cortex).

To this end, we use a Khepera IV robot (http://www.k-team.com/khepera-iv). The robot chassis can be considered as a "human skin", a metaphor that overlooks the fact that the input that robots can process, often limited to proximity sensors like IR or ultrasonic, as in our case, is very far from the complexity and the nuanced information human skin provides, such as texture, temperature, and pressure variations. Although efforts have been made to develop sensors mimicking biological features [1, 21], they may not align with the current capabilities of robots [3]. Although we use the IR sensors fitted around the robot's chassis to map the receptive field of the robot's body, we have developed a complex representation of touch (mechanoception and nociception) in the "sensory body" of the robot, in order to extract relevant tactile features to be transmitted to a biologically realistic artificial neural network. This neural network will then adapt to these external signals, shaping its overall organization.

2 The sensory body

This section describes the robot's "sensory body" used to model tactile sensations and the interaction between mechanoreceptors and nociceptors.

2.1 Tactile sensory fields

To model complex tactile sensing in our robot, we have developed a "sensory field" using proximity sensors, to better capture some of the complexity of human skin's tactile sensations. It is conceptualized through both its nominal and

actual forms, where sensor readings, relative to a nominal (undisturbed) position, assess deformations triggered by environmental interactions. This analysis not only quantifies these interactions but also provides a qualitative insight into the robot's tactile experience.

We employ the Khepera-IV robot, a compact circular robot fitted with eight evenly distributed InfraRed (IR) sensors around its chassis. To allow for a more detailed spatial analysis, we first interpolate additional values between the IR—the average of the readings of two consecutive sensors is interpolated twice between each pair of consecutive IR sensors, to enhance spatial resolution from 8 to 32 values. These interpolated values are then translated into polar coordinates, offering a nuanced understanding of sensory interactions. For visualization, these polar coordinates are further transformed into Cartesian coordinates, depicting the sensory field as a "blob". This representation effectively illustrates the sensory body's "deformation" (its changing, adaptable shape) in response to external stimuli, with a nominal position established to denote its "undisturbed" state (lack of sensory stimulation).

Our model also differentiates between nociceptors and mechanoreceptors, and aims to simulate the skin's elasticity and responsiveness by employing a dual-field approach to encapsulate their distinct responses to stimuli [22]. This distinction is crucial, as mechanoreceptors and nociceptors transmit signals at different speeds: whereas β fibers relay touch and vibration quickly (30-70 m/s), δ fibers, associated with pain, which conduct at slower speeds (5-30 m/s) [24].

2.2 Mechanoceptors

In humans, mechanoreceptors are crucial for detecting a broad spectrum of tactile stimuli; they are primarily found within the dermis layer of the skin [15, 14]. Our model mirrors this with the placement of IR sensor values in our defined sensory body (Fig. 1, A). They play a vital role in interpreting force, strain, and stress applied to skin, quantifiable through Hooke's Law ($F = k \cdot \Delta L$), which describes the linear relationship between the force applied and the elastic deformation of an object, and formulas for strain ($\epsilon = \frac{\Delta L}{L_0}$), stress ($\sigma = \frac{F}{A}$), and Young's Modulus ($E = \frac{\sigma}{\epsilon}$), which defines the stiffness of a material, with measurements in standard units of Newtons, Pascals, and dimensionless ratios.

The mechanotransduction pathway activates with these receptors' response to external forces, using Young's Modulus at each sensory point to determine activation levels. This data integrates with a neural network simulating the somatosensory cortex's response to tactile stimuli (Fig. 1, F). This model encapsulates the complex relationship between physical deformation and neural response, showcasing the encoding and processing of tactile information.

2.3 Nociceptors

Nociceptors, recognized as the sensors of pain [10], are sensitive to noxious stimuli, playing a critical role in the body's ability to detect and respond to potentially harmful conditions. These receptors are adept at discerning various

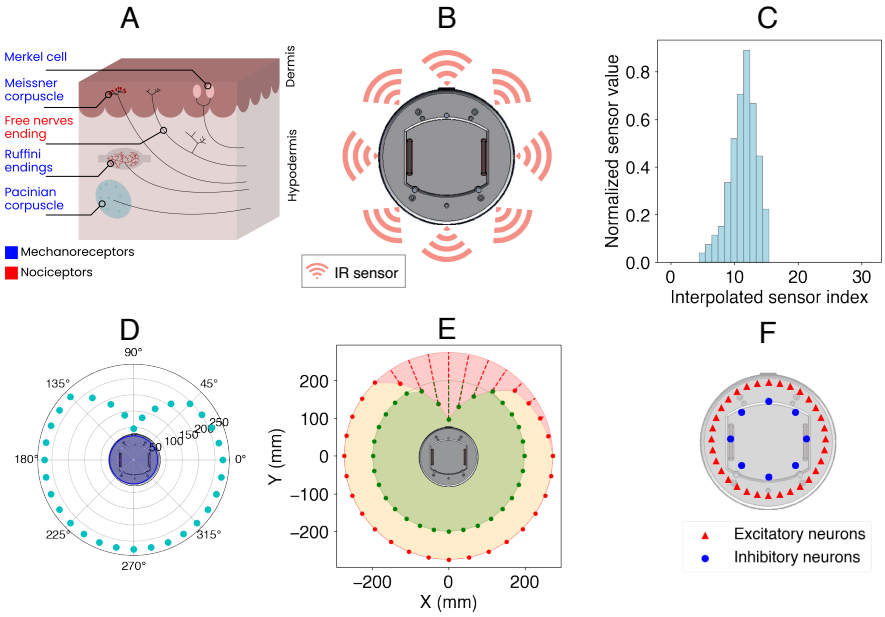

Fig. 1. (A) Shows four types of mechanoceptors (in blue) and nociceptive free nerve endings (in red) in the human hand, drawn after [16]. (B) Top view representation of a Khepera-IV robot with 8 IR sensors. (C) Normalized and interpolated IR sensor data from 8 to 32 values. (D) Polar coordinates from the data showing the robot's physical outline. (E) Representation of sensory body's deformed through pressure in Cartesian space; the red circle indicates the nominal position of mechanoceptors, the green circle marks the nominal nociceptors' position, illustrating proximity to the robot's body and a positional threshold. The yellow and green fields represent the "deformed" sensory and nociceptive layers, respectively. (F) Cortical neurons processing mechanoceptive information, with red circles for excitatory and blue for inhibitory neurons.

characteristics of stimuli, including intensity, duration, and even the type of the pain: whether it is sharp, throbbing, or burning.

Based on this understanding, we compute physical information on our sensory field deformation to distinguish touch events, drawing parallels between the nociceptors' functionality and our system's ability to interpret tactile data. This involves analyzing the diffuse or intense deformation of the blob, using a classification algorithm, the velocity of the touch, its duration, and the frequency of touch encounters. From our sensory body, we thus compute eight pieces of information across four physical aspects (deformation, velocity, frequency and duration), each with two classes, forming an 8-dimensional vector representing noxious stimuli for the neural network. This vector accounts for the speed difference between slower δ fibers (nociceptive) and faster β fibers (mechanoceptive). To account for this speed difference, we delay stimuli in time.

As depicted in Fig. 2, our methodology for computing nociceptive features begins by assessing the force exerted across the sensory field to evaluate deformation. This analysis helps us identify whether the contact is focused or disperse, categorized as intense or diffuse deformation respectively (Fig. 1, A & B). We then determine touch activation based on these deformations (Fig. 1, C), leading to the calculation of key tactile characteristics: frequency of touch events (Fig. 1, D & E), duration(Fig. 1, I & J), and velocity of deformation (Fig. 1, G & H).

3 Neural network model

To process sensory information from mechanoreceptors and nociceptors and to model the neuronal activity of the somatosensory cortex and the Anterior Cingulate Cortex (ACC), we employ a biologically inspired spiking neuronal network subject to synaptic plasticity. For more details on the model and implementation choices, see [4, 6].

3.1 Spiking neuronal network model

Throughout this study, we use a network of excitatory-inhibitory heterogeneous quadratic integrate and fire (QIF) neurons [11]. The network is composed of 80% of excitatory neurons and 20% of inhibitory neurons, as commonly accepted in the human cortex [20]. The inhibitory neurons are divided into two distinct populations: a population following Hebbian learning, and a population following anti-Hebbian learning (i.e. neurons that fire together, decoupled together).

Therefore, the evolution of the membrane potential V_i of each neuron ($i = 1, ..., N$) is described by the following equation:

$$\tau_m \dot{V_i} = V_i^2(t) + \eta_i + g_e S_i^e(t) + g_{hi} S_i^{hi}(t) + g_{ai} S_i^{ai}(t) + I_i(t) + \xi_i(t), \quad (1)$$

where synaptic inputs $S_i^e(t)$, $S_i^{hi}(t)$, and $S_i^{ai}(t)$ (excitatory, Hebbian inhibitory, and anti-Hebbian inhibitory, respectively) for neuron i are defined by:

$$\tau_d^{e(i)} \dot{S_i^{e(hi,ai)}} = -S_i^{e(hi,ai)} + \frac{\tau_d^{e(i)}}{N_{e(hi,ai)}} \sum_j^{N_{e(hi,ai)}} w_{ij} \delta(t - t_j), \quad (2)$$

where $\tau_m = 0.02$s is the membrane time constant, $\tau_d^e = 0.002$s and $\tau_d^i = 0.005$s the time decay of excitatory and inhibitory neurons, $\eta_i \sim \mathcal{N}(0.0, (\pi\tau_m)^2)$ the excitability parameter, $N = N_e + N_{hi} + N_{ai} = 100$, $N_e = 80$, $N_{hi} = 10$ and $N_{ai} = 10$ respectively the number of excitatory and Hebbian and anti-Hebbian inhibitory neurons, $g_e = 100$, $g_{hi} = 400$ and $g_{ai} = 200$ the global coupling strength for the excitatory neurons and Hebbian and anti-Hebbian inhibitory neurons. The coupling weights from neuron j to i is depicted by w_{ij}, t_j is the time of spike of the j-th neuron, and $\delta(t)$ is the Dirac delta function. Finally, $I_i(t) = \{0, (50\pi\tau_m)^2\}$ is an external input current and $\xi_i(t) \sim \mathcal{N}(0.0, (4\pi\tau_m)^2)$ is a Gaussian noise. We consider a fully connected network without self-connections.

3.2 Plasticity functions

Regarding the adaptation of the weights w_{ij}, we use spike-timing-dependent plasticity (STDP) rules that depend on the time difference $\Delta t = t_i - t_j$ between the last spikes of the post-synaptic neuron i and pre-synaptic neuron j. The plasticity functions $\Lambda^+(\Delta t)$ and $\Lambda^-(\Delta t)$ from Eqs. 3 for potentiation and depression respectively, depend on the nature of the pre-synaptic neuron.

$$\Lambda^+(\Delta t) = \begin{cases} \Lambda(\Delta t), & \text{if } \Lambda(\Delta t) \geq 0, \\ 0, & \text{if } \Lambda(\Delta t) < 0, \end{cases} \quad \Lambda^-(\Delta t) = \begin{cases} 0, & \text{if } \Lambda(\Delta t) \geq 0, \\ \Lambda(\Delta t), & \text{if } \Lambda(\Delta t) < 0. \end{cases} \tag{3}$$

For excitatory neurons we use a Hebbian STDP asymmetric function commonly used in the literature [7] described by Eq. 4.

$$\Lambda(\Delta t) = \begin{cases} A_+ e^{-\frac{\Delta t}{\tau_+}} - A_- e^{-\frac{4\Delta t}{\tau_+}} - f, & \text{for } \Delta t \geq 0, \\ A_+ e^{\frac{4\Delta t}{\tau_-}} - A_- e^{\frac{\Delta t}{\tau_-}} - f, & \text{for } \Delta t < 0, \end{cases} \tag{4}$$

with the time constants $\tau_+ = 0.02$s and $\tau_- = 0.05$s, the amplitudes $A_+ = 5.296$ and $A_- = 2.949$. The forgetting term $f = 0.1$ allows to have a constant small depression of the weights whatever the spike timing difference. It models the natural, constant and slow forgetting of memories [13].

For Hebbian (anti-Hebbian) inhibitory neurons we use a Hebbian (anti-Hebbian) STDP symmetric function [23, 17] described by Eq. 5.

$$\Lambda(\Delta t) = \pm A(1 - (\frac{\Delta t}{\tau})^2) e^{\frac{-\Delta t^2}{2\tau^2}} \mp f, \tag{5}$$

with time constant $\tau = 0.1$s, amplitude $A = 3$ and forgetting term $f = 0.1$.

3.3 Adaptation of synaptic weights

The evolution of the synaptic weights, which remain continually subject to adaptation, unlike more conventional learning systems, follows this ordinary differential equation:

$$\tau_l \dot{w_{ij}} = (-1)^{a_q} [\tanh(\lambda(w_q^l - w_{ij})) * \Lambda_q^+(\Delta t) + \tanh(\lambda(w_{ij} + w_q^u)) * \Lambda_q^-(\Delta t)] \tag{6}$$

where q denotes if the pre-synaptic neuron is excitatory $q = e$ or Hebbian (anti-Hebbian) inhibitory $q = hi$ ($q = ai$), for excitatory (inhibitory) neurons we set $w_q^l = 1$ ($w_q^l = 0$) and $w_q^u = 0$ ($w_q^u = 1$), thus ensuring that the excitatory (inhibitory) couplings are defined in the following interval $w_{ij} \in [0 : 1]$ ($w_{ij} \in [-1 : 0]$). Moreover, $a_e = 2$ and $a_{hi} = a_{ai} = 1$, thus for inhibitory synapses, the plasticity functions $\Lambda^+(\Delta t)$ and $\Lambda^-(\Delta t)$ are inverted and multiplied by -1 since potentiation (depression) of inhibitory weights makes them converge towards -1 (0). Finally, $\tau_l = 0.2$s is the learning time scale for the adaptation.

4 Experiments and Results

4.1 Experimental Setup

A Khepera IV robot was placed on a table in the robotics laboratory. A human interacted with the robot, stimulating its IR sensors by inducing contact within the sensory field area with his hand (as shown in 2) in the following experimental conditions. Three repetitions of touch tests focusing on four metrics were carried out: Speed (Slow, Fast), Frequency (Low, High), Duration (Short, Long), and Intensity (Diffuse, Intense). For each metric, sensors underwent individual testing under each condition, resulting in a total of 64 tests (8 sensors x 4 metrics x 2 conditions). To mitigate bias, both the order of conditions and the sensors were randomized. Each touch event was separated by 1 second, with sensor data captured at a frequency of 100Hz, ensuring a comprehensive dataset. The inclusion of randomization in sensor and condition order aimed to prevent any sequential bias and ensure the robustness of the experimental results. The experiment lasted 20 minutes, and data were collected throughout. The experiment was run 5 times, with similar results. Below we discuss a representative run.

4.2 Results

Nociceptors & Mechanoceptors output. In Fig. 2, we can observe the output of the nociceptive vector and of the physical information we used to compute it in a specific time windows between 125 and 150 seconds. Mechanoceptor vector has been computed as described in 2.2. These data are sent to the neuronal model.

Dynamics during learning. We first describe the dynamics of the network during learning of external sensory stimuli in Fig. 3, A. First, we observe that neurons associated with mechanoreceptors (excitatory neurons 64 to 127 and inhibitory neurons 144 to 159) respond to tactile input slightly earlier than neurons associated with nociceptors (excitatory neurons 0 to 63 and inhibitory neurons 128 to 143). This time delay between the information from the two types of sensor stems from the beta (for mechanoreceptors) and delta (for nociceptors) fibers, which transmit sensory information to the two cortical areas at different speeds.

In the somatosensory area (see light spikes), a touch on the robot is characterized by an increase in the firing rate of neurons (excitatory and inhibitory)

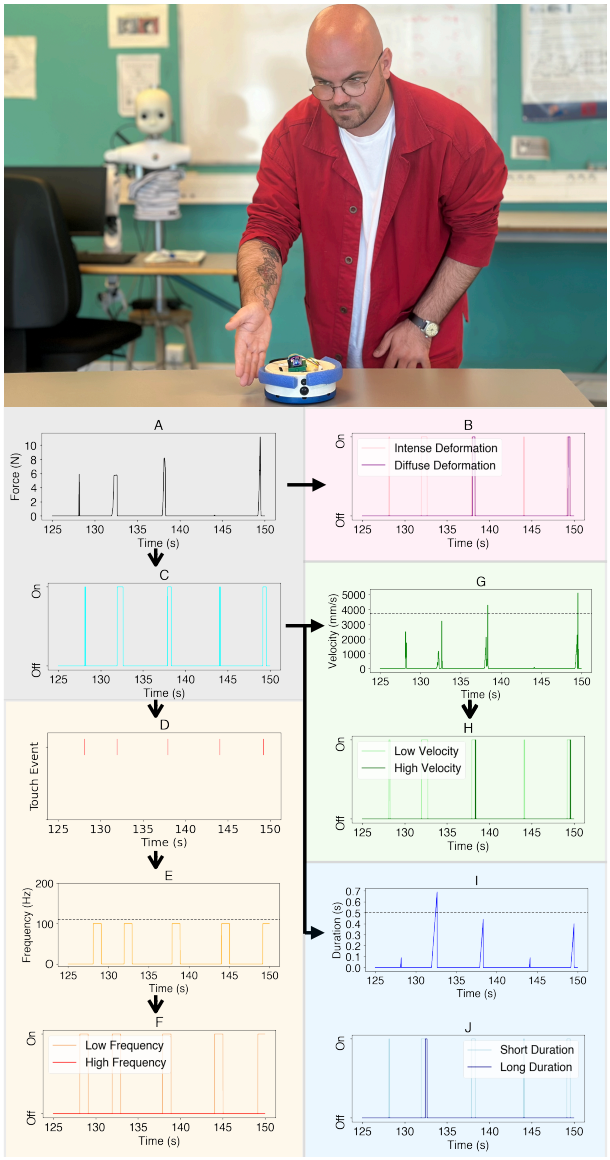

Fig. 2. Picture of our experimental setup (top), and Dynamic Interactions and Time-Based Analysis of Tactile Sensory Events in a Nociceptive Model. Black arrows indicate the directional interactions between different tactile sensory events within the same time window. (A) Mean force applied to the nociceptive field over time. (B) Partitioning of deformation on the nociceptive blob over time. (C) Activation of touch on the blob over time, true if a certain amount of force is applied to the blob. (D) Touch event over time. (E) Frequency of touch in Hz over time. (F) Separation of frequency bands over time. (G) Velocity of touch in mm/s over time. (H) Segregation of velocity bands over time. (I) Duration of touch over time. (J) Division of duration bands over time.

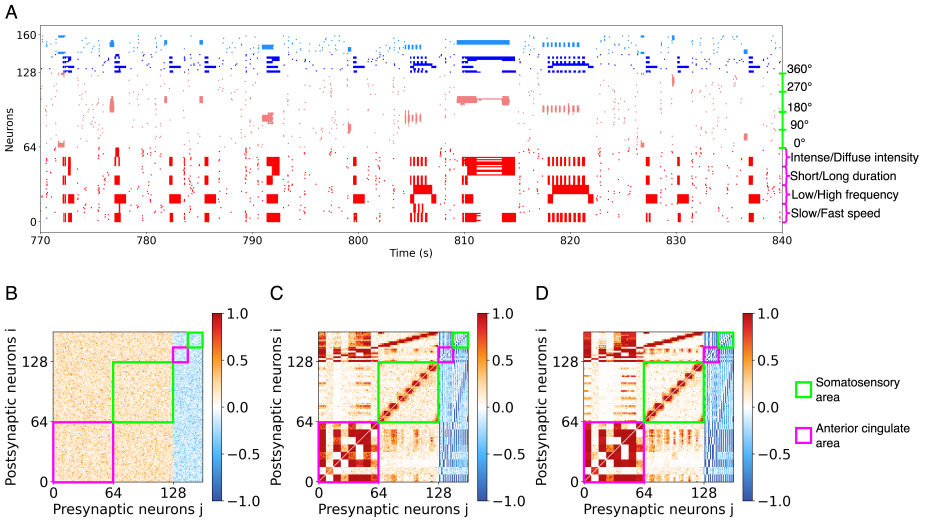

Fig. 3. Neuronal simulation of touch stimulation. (A) The raster plot displays the firing times of excitatory (red dots) and inhibitory (blue dots) neurons during the simulations. Dark red (blue) dots represent spikes in the anterior cingulate cortex (nociceptors), while light dots represent spikes in the somatosensory cortex (mechanoreceptors). (B,C,D) The matrices represent the connection weights between neurons at the beginning, middle and end of the simulation. The color denotes if the connection is excitatory (red) or inhibitory (blue) or absent (white). The magenta area represents the ACC with touch features, while the green area represents the somatosensory cortex with locations of touch.

associated with a specific location on the robot's body. Thus, a more spread contact will activate more neurons than a more targeted contact. In addition, a deeper touch will increase neuron activity more than a softer touch.

On the side of the anterior cingulate area (see dark spikes), neurons (excitatory and inhibitory) increase their activity in the presence of particular touch features such as frequency bands, duration bands, deformation shapes and velocity bands. In this way, certain neurons are never activated at the same time, given the opposite nature of the features they encode (e.g. intense versus diffuse deformation). Conversely, certain features can be activated at the same time when they are not incompatible (e.g. a diffuse, long and low-frequency touch). In addition, it should be noted that some feature neurons activate only after other features have been activated. For example, a touch must be perceived as short before it can be considered long.

Resulting weight connectivity. This learning leads to the formation of particular structures in the weights connectivity of Fig. 3, B to D. Firstly, at the global level, we observe the formation of two modular structures, where excitatory neurons associated with the same sensory receptors (either nociceptors in ma-

genta or mechanoreceptors in green) share strong connections, while connections between the two sensory areas are sparse and weak. This segregation between cortical areas is made possible by the beta and delta fibers described above, which prevent temporal correlations between information from nociceptors and mechanoreceptors, and hence their structural reinforcement.

In the area associated with mechanoreceptors (in green), we find that neurons associated with physically close sensors are strongly connected, while connections between distant areas are essentially suppressed. In other words, we obtain the formation of a kind of ring connectivity representing the robot's body.

Concerning the nociceptors area (in magenta), we can see that neurons coding for contradictory information (e.g. low and high frequencies) are totally decoupled. Nevertheless, some distinct feature neurons are strongly connected, showing that certain types of touch are characterized by different features. In particular, we find that some feature neurons, such as those associated with low frequency touch, share connections with all other feature neurons. Indeed, these features almost always remain active, which also explains the few weak connections between the two cortical areas.

5 Discussion & Conclusion

In this paper, we have presented a sensory body model for a mobile robot able to capture complex information about touch, including painful touch, from few data. We further investigated the coding of nociceptive features in an artificial neural model of Anterior Cingulate Cortex, a brain region associated with processing emotions and pain [25]. In the representation that emerged, we observed correlations and decorrelations between some nociceptive features extracted from different types of noxious stimuli, suggesting specific coding mechanisms.

Using a Khepera IV robot, we modeled a specific sensory body and tested various noxious stimuli designed to elicit distinct responses. The observed correlations and decorrelations between specific nociceptive inputs imply that some features co-activate, potentially encoding and discriminating different types of noxious stimuli. For example, in skin, pressure, scratch, and pinch stimuli activate distinct features. These observations support Acuña's [2] description of nociceptive coding in the ACC.

We also investigated how tactile information from nociceptors and mechanoreceptors can be learned by an artificial neural network to form two distinct areas, comparable to what can be observed in biology with the anterior cingulate cortex and the somatosensory cortex. This highlights the segregation of information, with the specialization of brain regions for specific tasks or modalities [29]. These results echo those obtained by Bergoin et al. in [5, 6] with simpler stimuli.

Further, the ACC and somatosensory cortex individually provide information on the characteristics of the touch (what and how) and on its location (where). More precisely, in our somatosensory network, we found that neurons coding for physically close robot body parts were more strongly connected than those for

distant ones. This reminds us of the concept of semantic memory, where we find an association between mental representations and topology [29].

Our model contributes to the explainability of robot behavior, since, given that the neural network is able to react to particular features and the location of touch, we could read these neural activities directly and associate them with particular behaviors or reflexes.

In future work we could learn these associations and teach the robot to link certain features with types of pain or pleasure and particular movements. Finally, the neural network used would allow us to carry out experiments in more complex and changing environments, and assess the ability of the model to maintain continual learning without catastrophic forgetting of memories.

Acknowledgement. LLH and this research are supported by an INEX Chair in Neuroscience and Robotics to LC.

References

1. Abdelwahed, M., Zerioul, L., Pitti, A., Romain, O.: Using novel multi-frequency analysis methods to retrieve material and temperature information in tactile sensing areas. Sensors **22**(22), 8876 (2022)
2. Acuña Miranda, M.A., Kasanetz, F., De Luna, P., Falkowska, M., Nevian, T.: Principles of nociceptive coding in the anterior cingulate cortex. Proceedings of the National Academy of Sciences of the USA-PNAS **120**(23) (2023)
3. Bagnato, C., Takagi, A., Burdet, E.: Artificial nociception and motor responses to pain, for humans and robots. In: 2015 37th Annual International Conference of the IEEE Engineering in Medicine and Biology Society (EMBC). pp. 7402–7405. IEEE (2015)
4. Bergoin, R.: The role of inhibitory plasticity in the formation and the long-term maintenance of neural assemblies and memories. Ph.D. thesis, CY Cergy Paris Université; Universitat Pompeu Fabra (2023)
5. Bergoin, R., Torcini, A., Deco, G., Quoy, M., Zamora-Lopez, G.: Inhibitory neurons control the consolidation of neural assemblies via adaptation to selective stimuli. Scientific Reports **13**(1), 6949 (2023)
6. Bergoin, R., Torcini, A., Deco, G., Quoy, M., Zamora-López, G.: Emergence and long-term maintenance of modularity in spiking neural networks with plasticity. arXiv preprint arXiv:2405.18587 (2024)
7. Bi, G.q., Poo, M.m.: Synaptic modifications in cultured hippocampal neurons: dependence on spike timing, synaptic strength, and postsynaptic cell type. Journal of neuroscience **18**(24), 10464–10472 (1998)
8. Christensen, A., Corey, D.: Trp channels in mechanosensation: direct or indirect activation? Nature Reviews Neuroscience **8**, 510–521 (2007)
9. Cobo, R., García-Piqueras, J., García-Mesa, Y., Feito, J., García-Suárez, O., Vega, J.A.: Peripheral mechanobiology of touch—studies on vertebrate cutaneous sensory corpuscles. International Journal of Molecular Sciences **21**(17) (2020). https://doi.org/10.3390/ijms21176221
10. Dubin, A.E., Patapoutian, A., et al.: Nociceptors: the sensors of the pain pathway. The Journal of clinical investigation **120**(11), 3760–3772 (2010)

11. Ermentrout, B.: Type i membranes, phase resetting curves, and synchrony. Neural computation **8**(5), 979–1001 (1996)
12. Gilson, M., Deco, G., Friston, K.J., Hagmann, P., Mantini, D., Betti, V., Romani, G.L., Corbetta, M.: Effective connectivity inferred from fmri transition dynamics during movie viewing points to a balanced reconfiguration of cortical interactions. Neuroimage **180**, 534–546 (2018)
13. Hardt, O., Nader, K., Nadel, L.: Decay happens: the role of active forgetting in memory. Trends in cognitive sciences **17**(3), 111–120 (2013)
14. Johnson, K.O.: The roles and functions of cutaneous mechanoreceptors. Current Opinion in Neurobiology **11**(4), 455–461 (2001)
15. Julius, D., Basbaum, A.: Molecular mechanisms of nociception. Nature (2001)
16. Kandel, E.: Principles of Neural Science. McGraw-Hill, New York (2013)
17. Lamsa, K.P., Heeroma, J.H., Somogyi, P., Rusakov, D.A., Kullmann, D.M.: Anti-hebbian long-term potentiation in the hippocampal feedback inhibitory circuit. Science **315**(5816), 1262–1266 (2007)
18. L'Haridon, L., Cañamero, L.: The effects of stress and predation on pain perception in robots. In: 2023 11th International Conference on Affective Computing and Intelligent Interaction (ACII). pp. 1–8. IEEE (2023)
19. Maniscalco, U., Infantino, I.: An artificial pain model for a humanoid robot. In: De Pietro, G., Gallo, L., Howlett, R.J., Jain, L.C. (eds.) Intelligent Interactive Multimedia Sys and Services 2017. pp. 161–170. Springer Int Publishing (2018)
20. Markram, H., Toledo-Rodriguez, M., Wang, Y., Gupta, A., Silberberg, G., Wu, C.: Interneurons of the neocortical inhibitory system. Nature reviews neuroscience **5**(10), 793–807 (2004)
21. Parvizi-Fard, A., Salimi-Nezhad, N., Amiri, M., Falotico, E., Laschi, C.: Sharpness recognition based on synergy between bio-inspired nociceptors and tactile mechanoreceptors. Scientific reports **11**(1), 2109 (2021)
22. Pawlaczyk, M., Lelonkiewicz, M., Wieczorowski, M.: Age-dependent biomechanical properties of the skin. Advances in Dermatology and Allergology/Postepy Dermatologii i Alergologii **30**(5), 302–306 (2013)
23. Perez, Y., Morin, F., Lacaille, J.C.: A hebbian form of long-term potentiation dependent on mglur1a in hippocampal inhibitory interneurons. Proceedings of the National Academy of Sciences **98**(16), 9401–9406 (2001)
24. Perl, E.: Myelinated afferent fibers innervating the primate skin and their response to noxious stimuli. Journal of Physiology **197**, 593–615 (1968)
25. Rainville, P., Duncan, G.H., Price, D.D., Carrier, B., Bushnell, M.C.: Pain affect encoded in human anterior cingulate but not somatosensory cortex. Science **277**(5328), 968–971 (1997)
26. Scannell, J.W., Blakemore, C., Young, M.P.: Analysis of connectivity in the cat cerebral cortex. Journal of Neuroscience **15**(2), 1463–1483 (1995)
27. Vallbo, A.B., Johansson, R.S., et al.: Properties of cutaneous mechanoreceptors in the human hand related to touch sensation. Hum neurobiol **3**(1), 3–14 (1984)
28. Wang, L., Ma, L., Yang, J., Wu, J.: Human somatosensory processing and artificial somatosensation. Cyborg and Bionic Systems (2021)
29. Zamora-López, G., Zhou, C., Kurths, J.: Exploring brain function from anatomical connectivity. Frontiers in neuroscience **5**, 83 (2011)